
A numerical simulation of measured transient temperatures in the walls, floor and surrounding soil of a buried structure

A numerical simulation

405

Received May 1998
Revised November 1998
Accepted December 1998

M.H. Adjali

Research in Building Group, University of Westminster, London, UK

M. Davies

*Department of Mechanical Engineering, Brunel University,
Middlesex, UK, and*

J. Littler

Research in Building Group, University of Westminster, London, UK

Keywords Buildings, Flooring, Heat transfer, Structures

Abstract *Presents the results of a numerical simulation of measured heat transfer through a region surrounding a buried structure. The model applied in the study is a widely used whole building thermal simulation program of a type which predicts the thermal response of structures for building services requirements. A multi-dimensional numerical conductive heat transfer module has been added to this program but this does not specifically address earth-contact heat flows. This work attempts to assess the accuracy of the overall package when predicting earth-coupled heat transfer. It is common practice in the field of building services not to use specific earth-contact models and so it is important to assess the likely errors thus involved. The predictions of the finite-volume model are compared with one year of data from a basement test facility. The results are analysed using the Differential Sensitivity Analysis method and an attempt is made to correlate predictive errors with periods of rainfall and snow coverage. It seems that a purely conductive model may be capable, given accurate input data, of satisfactorily predicting the transient temperature variations in the soil/concrete envelope surrounding this structure for the period of the year when no snow coverage is present. However, if one is to accurately model regions of earth-contact (particularly at shallow depths) in a climate in which rainfall and snow are significant then these influences should be explicitly modelled.*

Introduction

Background

In a well-documented survey Claridge (1987) noted that in the USA a waste of about \$5-\$15 billion a year is attributable to heat transfer to the ground. A drive towards improved above-ground insulation, as a result of the energy crisis of the early 1970s, led to the heat losses associated with earth-contact becoming proportionally more important. Shipp (1983) reported that for instance in Ohio,

The financial support of the Engineering and Physical Sciences Research Council (grant ref. GR/K77105) is gratefully acknowledged. The authors would also like to thank Dr Louis Goldberg from Lofrango Engineering, Minneapolis, for supplying the FTF data set.

International Journal of Numerical
Methods for Heat & Fluid Flow,
Vol. 9 No. 4, 1999, pp. 405-422.
© MCB University Press, 0961-5539

USA, an uninsulated basement can account for 67 per cent of the total envelope load when the above-ground part of the building is well insulated. Other studies by Claesson and Hagentoft (1991) and Bahnfleth (1989) claim that in cold climates the heat loss to the ground might be responsible for up to one-third or even a half of total heat losses.

Until recently, none of the major computer tools used to predict the thermal response of structures for building services requirements (e.g. APACHE, DOE-2.1, ESP, SERIRES, TAS, TRNSYS, etc.) treated the ground coupling problem in detail. In order to overcome this deficiency the trend seems to be towards the integration of dedicated modules into such codes. Recent work includes the addition of a three-dimensional conductive heat flow module to APACHE by Davies (1994) at the University of Westminster (UK) and the development of a module within the environment of TRNSYS by Mihalakakou *et al.* (1995) at the University of Athens (Greece) to enable it to predict the three-dimensional ground temperature profile.

The treatment of earth-contact heat flows is complex. In a recent paper, Davies *et al.* (1995) showed the importance of multi-dimensional heat flow modelling. Three simulation modes (1, 2 and 3D) were used to predict the annual heating loads of an above-ground structure. The author found a discrepancy of 22 per cent between the 2D and 3D simulations and 41 per cent between the 1D and 3D simulations. Unfortunately, most of the works undertaken on this subject simplify the problem to a one- or in the best case to a two-dimensional process. This can be satisfactory in some cases but it has been shown by Muncey *et al.* (1978) that it is not appropriate in certain circumstances e.g. detached domestic buildings. Other modelling by Saxhof *et al.* (1993) has been done in the context of the "Danish Advanced Solar Low Energy Building" program, and a discrepancy of over 50 per cent was found between 1D and 2D heat load simulations. A similar study by Walton (1987) indicated errors up to 50 per cent in estimating heat loss from rectangular basements and slabs into the ground using two-dimensional and three-dimensional calculations. The heat flow between the building and the earth can thus no longer generally be realistically considered as a one-dimensional process.

Generally, for simplicity, the most common practice in the mathematical treatment is to consider constant thermophysical properties. However, the soil is generally unhomogeneous and thermophysical properties vary with temperature and moisture. Complications thus arise from the non-linearity of the problem. Coupled heat and moisture transfer in the ground has been studied for several years at the Cardiff School of Engineering (UK), e.g. Thomas (1987), and at this time its effect on heat flows around buildings is under investigation. It appears from previous works e.g. Van Den Brink and Hoogendoorn (1983) that the moisture effect can be neglected in certain cases e.g. soil of low permeability. Lloyd (1994) concluded that the variation in

moisture content was negligible in the 2m immediately under the ground floor slab studied. In general though, it is unclear under which circumstances such coupling may be ignored.

Boundary conditions can also be a limitation to realistic modelling when complex geometry structures are studied. Additionally, the long term transient nature of the problem due to the high thermal capacity of the earth must be addressed. It is clear then that the physical process is very difficult to model satisfactorily without resorting to numerical techniques.

Aim of this work

The work reported here is part of a wider project, the aim of which, in part, is to investigate which is the most suitable type of simulation tool to use for any given instance of earth-coupling. This phase of the project involves modelling a variety of different structures using a purely conductive, transient, three dimensional model and identifying how successful this model is. Any periods of data not modelled satisfactorily by the model will then be passed to a coupled heat and moisture model (Cardiff School of Engineering) and further simulation work then carried out to assess the importance of this coupling effect. The ability of a non-specific “earth-contact” model to satisfactorily simulate this process will have thus been assessed.

This paper then, reports on the testing of this numerical model using the APACHE simulation program to which a module incorporating the model has been added. The testing utilises data obtained from a basement test facility specifically set up to investigate earth-coupled heat flows and to provide data against which to test models. The data set is ideal as it involves periods of significant rainfall and snow coverage. The assumption was that periods of snow coverage would not be modelled well and that perhaps the most interesting part of the investigation would relate to the ability of the model to cope with periods of rainfall.

Experimental data

The thermal performance of an uninsulated test module has been measured for a period covering four heating seasons. This experiment was carried out at the University of Minnesota, Minneapolis, USA and is known as the Foundation Test Facility (FTF). The module has been instrumented extensively, both inside (26 internal temperature and heat flux measurement locations) and in the envelope (733 probe locations). No measurements in the surrounding ground are available. The floor of the structure is square ($5.89 \times 5.89 \text{ m}^2$) and the bottom of the walls is 2.03 m below the ground surface for a total height of 2.49 m, see Figure 1. The floor (of thickness 0.1 m) and the walls (of thickness 0.3 m) are both concrete with a thermal conductivity of $1.82 \text{ W m}^{-1} \text{ K}^{-1}$. The ceiling is well insulated and has been considered as an adiabatic boundary for the purpose of this study (U-value of $0.007 \text{ W m}^{-2} \text{ K}^{-1}$). The module is heated by the means of two U-shaped electric resistances and the internal temperature is

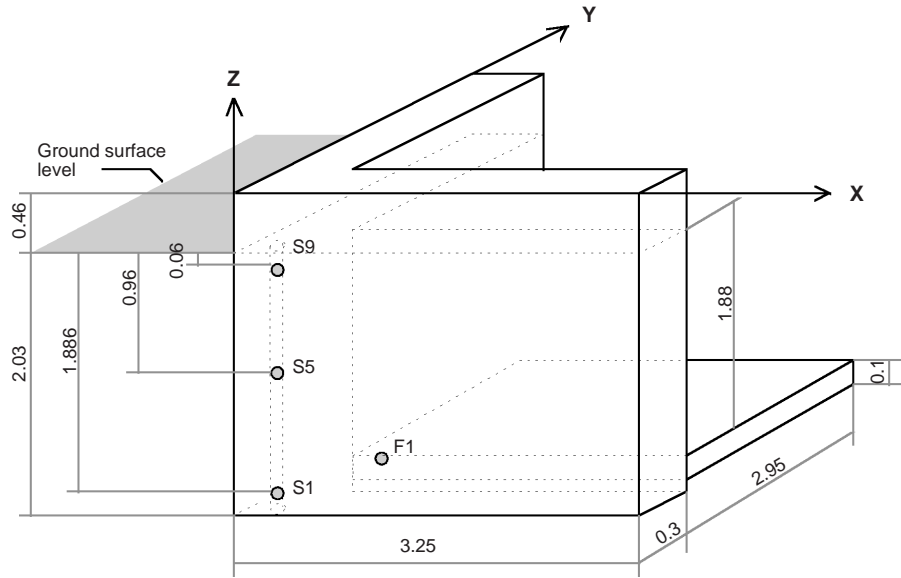


Figure 1.
One quarter of the FTF
module showing
thermocouple locations
(all dimensions in m)

controlled to a minimum set-point of 20°C and allowed to “float” above this temperature.

Figure 1 also shows the position of the temperature probes that relate to the simulated data presented in this study. Note that the thermocouple positions F1, S1, S5 and S9 reported in this work are located at the corner of the structure in an attempt to involve regions of three-dimensional heat flow. F1 is located 0.006 m below the slab surface at the internal corner of the structure. S1, S5 and S9 are all located at the corner soil/concrete interface. S1 is at a depth of 1.886 m, S5 at a depth of 0.96 m and S9 at a depth of 0.06 m.

The soil is settled with several layers, each one with specific thermophysical properties. Soil conductivities were determined using Johansen’s method, which, according to a comparative study by Farouki (1986) of different techniques, provides the best estimate for degrees of saturation greater than 0.2 (which is precisely the case of the FTF site). The thermal conductivity is a function of soil dry density, porosity and saturation ratio. Table I gives the material properties used in the simulation work.

The period identified as the time interval for the simulation is one year from 1 April 1990 to 31 March 1991. During this year the heating system was turned off for approximately five and a half months (from 8 June 1990 to 8 November 1990).

In this work the terms “spring”, “summer”, “autumn” and “winter” are used to describe periods of the simulated year (“spring” beginning 1 April 1990). The maximum daily average air temperature at the test site is 30°C and the minimum is -25°C. The most consistent precipitation is in the “spring” period followed by the “summer” and snow is present on the ground on most days from the end of the “autumn” period to the end of “winter”. Each of the four periods has a high percentage of clear days.

	Depth below ground (m)	Conductivity (W/m.K)	Heat capacity (J/kg.K)	Density (kg/m ³)
Surface layer – agricultural silt	0-0.76	0.94	2322	1611
Backfill – uniform sand	0-0.45	1.15	2322	1611
	0.45-0.76	0.96	1990	1506
	0.76-1.06	1.18	1722	1810
	1.06-1.37	1.00	1638	1836
	1.37-1.67	0.92	1615	1863
	1.67-1.98	1.87	1970	2014
	1.98-wall bottom	1.14	1682	1906
Undisturbed soil	0-0.45	1.14	2322	1611
	0.45-0.76	0.96	1990	1506
	0.76-1.06	1.15	1722	1810
	1.06-1.37	0.97	1638	1836
	1.37-1.67	0.88	1615	1863
	1.67-1.98	1.83	1970	2014
Concrete	1.98-deep ground	1.09	1682	1906
		1.82	653	2242

Table I.
Material properties used in simulation work

Theory and description of numerical model

A module has recently been developed by Davies *et al.* (1994) and added to the whole building thermal simulation program APACHE to enable it to model multi-dimensional conductive heat transfer. It is not a dedicated “earth-contact” module and hence does not model transpirative or evaporative effects at external surfaces. Neither can it model the effect of snow coverage and it makes the simplification of considering only material thermal isotropy. Details of the module, together with the tests applied to it (empirical, analytical and inter-model) may be found elsewhere (Davies, 1994). The work reported here is based on this three-dimensional heat conduction model. The numerical solution has been developed to solve transient linear problems. The governing equation is then:

$$\nabla^2 T = \frac{\rho c}{\lambda} \cdot \frac{\partial T}{\partial t} \quad (1)$$

The governing equation is discretised using techniques based on the work of Patankar (1980) and the finite-volume model can solve either the explicit or implicit forms. See Davies (1994) for a detailed account of the model. A brief description of the boundary node treatment follows.

Internal wall boundary

APACHE uses the binary star radiant-convective scheme as described by Davies (1990), in which each wall node is connected to both a radiant and air temperature point. The radiant point is defined such that the flow of heat from that point to a specific node is equal to the total flow of heat by longwave radiation from every other surface node in the room to that specific node. The

air point is simply the temperature of the (assumed fully mixed) air in a room that would be measured by a sensor shielded from the effects of longwave and shortwave radiant fields.

External surface boundary

External surfaces (walls and soil) interact with the external conditions via a “Solair” temperature defined as follows:

$$T_{\text{SOLAIR}} = T_{\text{OA}} + \text{SR}[(\text{DIR} + \text{DIF})\alpha - \epsilon \cdot \text{RADLWS}(\text{SLP})]$$

where:

- T_{OA} experimentally obtained outside air temperature (°C)
- DIR experimentally obtained direct radiation incident on surface (W/m²)
- DIF experimentally obtained diffuse radiation incident on surface (W/m²)
- RADLWS (SLP) a function which calculates the longwave radiation from a surface of slope SLP. It is a linear approximation based on the relevant equation from the *CIBSE Guide* (1986)

The values of the surface absorptivity α , emissivity ϵ and resistance SR are respectively 0.5, 0.9 and 0.06 m²K/W.

Simulation work

Discretised domain

A portion of the domain used to represent the walls, floor and surrounding earth is shown in Figure 2. Note that the boundaries extend to 10 m from the walls (see next section) and hence are not shown at this scale. The FTF module has two planes of symmetry and thus one quarter of the structure and surrounding soil is modelled with 39,888 nodes. The grid has variable space steps in the three directions; in general the closer a region to the concrete structure the finer the grid. The need for some nodes to coincide with the positions of the thermocouples in the wall and the floor also influenced the format of the mesh. Figure 2 shows typical grid spacings for the x and z directions. A time step of 120 seconds is used and the explicit form solved.

Boundary conditions

“Far field” boundaries were placed at 10 m from the walls of the structure. These boundaries were assumed to be adiabatic based upon sensitivity studies performed for a similar structure by Muncey *et al.* (1978). Other workers, e.g. Bahnfleth (1989), have also used similar boundaries for such structures. The external boundary conditions are hourly measured air temperatures and incident solar radiation incorporated into T_{SOLAIR} (see previous section on External surface boundary). The internal boundary conditions are hourly measured air temperatures. Figure 3 shows the T_{SOLAIR} and internal air

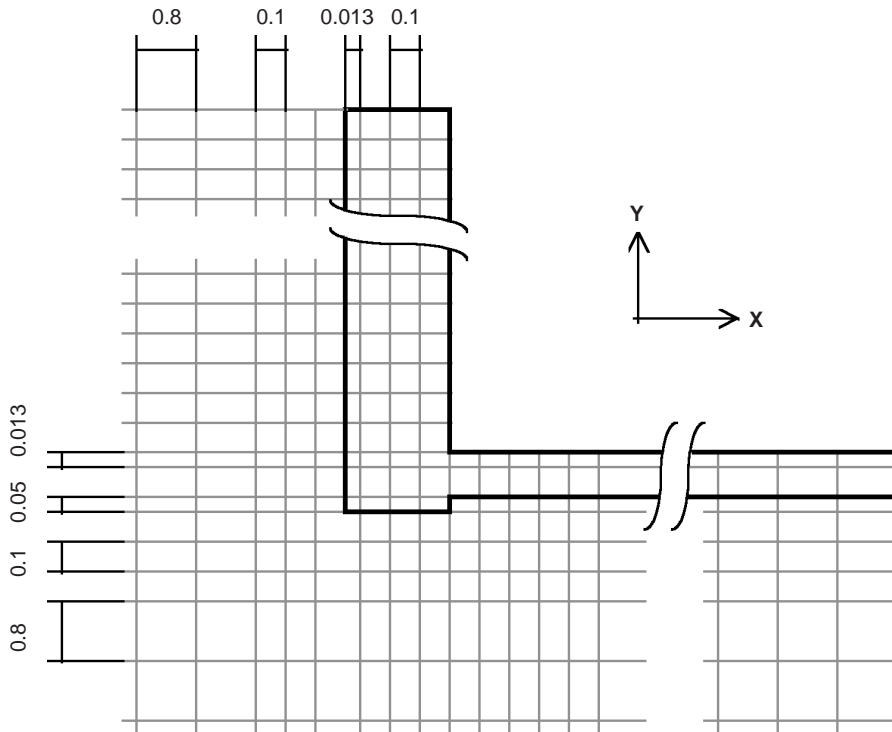


Figure 2. Finite difference grid (all dimensions in m, not to scale)

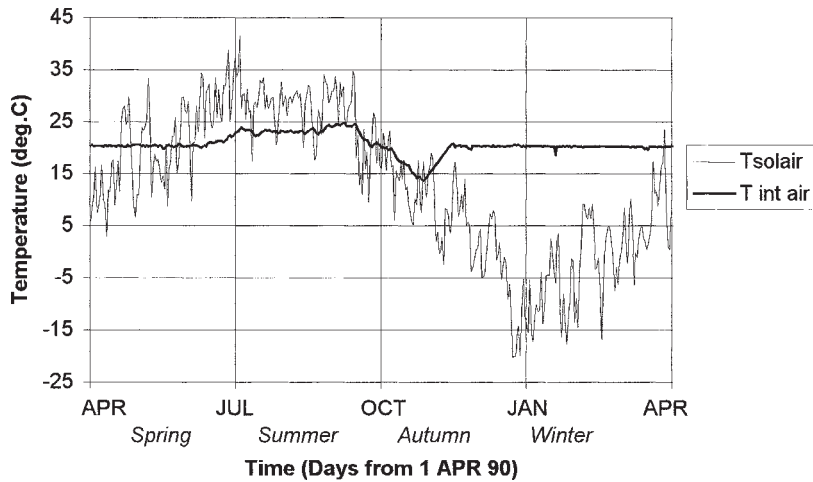


Figure 3. Daily mean internal air and T solair temperatures

boundary conditions ($T_{int\ air}$) as a function of time over the simulation period. Hourly internal “radiant” temperature boundary data were not available and so this was calculated by the model using the binary star radiant-convective scheme (see previous section on Internal wall boundary).

Pre-conditioning

Initial measured data were not available for the whole of the finite-volume domain. Indeed, data were restricted to the walls of the structure. Therefore the domain was initialised with a nominal 12°C and then allowed to be pre-conditioned for a period before the simulation proper was said to have begun. At the end of this period the domain was assumed to have achieved a dynamic equilibrium. In order to assess the necessary length of this pre-conditioning period, runs were performed in which at the end of an annual simulation the temperature of each node was stored and used as the initial condition for another year of simulation using the same boundary conditions. The predictions of year 1 were then compared with those of year 2. Whilst this is physically unrealistic to the extent that the same weather conditions are being used for both years, the point at which the two temperatures converge gives an indication of the length of the necessary pre-conditioning period. Example plots are shown for the two nodes F1 and S5 (Figures 4 and 5) where DT is the daily mean discrepancy between the year 1 and year 2 predictions. For the S5 node, after a period of 100 days, the discrepancy is less than 0.25°C. As stated above, this is not the “true” discrepancy as the same weather has been used in the two years, but this gives an indication that 100 days may be a reasonable period at which to assume dynamic equilibrium has been achieved. The F1 node discrepancy quickly becomes smaller than that of the S5 node due to it being more closely coupled with the measured internal air boundary condition.

Results

Note that in each case:

- approximately, the first 100 days are assumed to be a pre-conditioning period and this period is also included in the results;

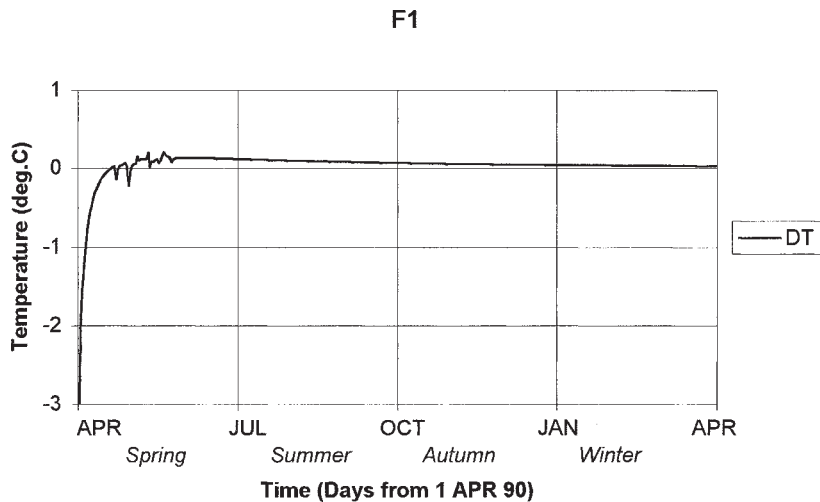


Figure 4.
Daily mean discrepancy between year 1 and year 2 predictions (node F1)

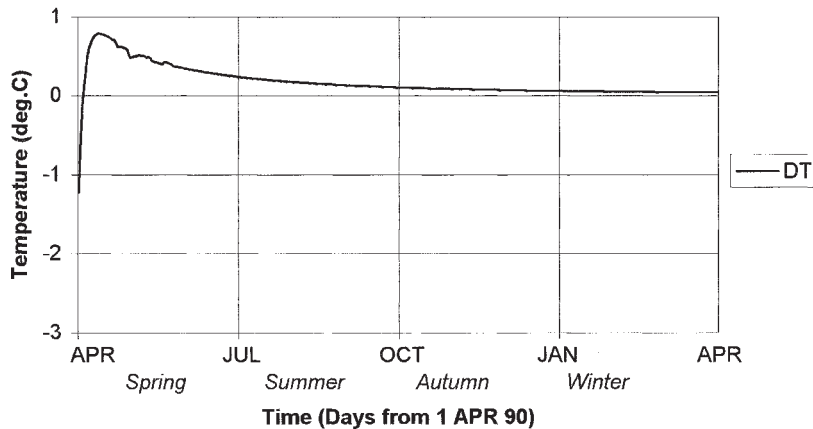


Figure 5.
Daily mean discrepancy
between year 1 and year
2 predictions (node S5)

- temperatures are daily means;
- if the daily hourly experimental data had any corrupted hours then those days means have been removed from the plots; and
- the simulation begins at 1 April 1990 i.e. “spring”.

In order to study the “spring” period in a meaningful manner an additional suitable pre-conditioning period would be required. The period of experimental data available for this current work dictated the simulation start date of 1 April 1990. The short period of data prior to this start date was not suitable for use in pre-conditioning due to the presence of snow on the ground and the inability of the model to take account of this phenomenon.

The main period of interest then is approximately the 115 days from the end of the pre-conditioning period to the first snow laying on the ground. This interval incorporates the “summer” period and some of the “autumn” period. During this time it will be possible to assess whether the conductive model is capable of simulating a period during which rainfall is quite frequent. After this period it was assumed that the model would be unable to successfully simulate the FTF module due to the presence of snow on the ground and the lack of a facility in the model to take this effect into account.

Daily mean temperatures for each node

In this section the Root Mean Square (RMS) errors of the simulated versus experimental daily mean temperatures are presented. Figure 6 shows that for node F1 good agreement is achieved in the “summer” (RMS error = 0.19°C) but agreement is poorer in “autumn” (RMS error = 1.36°C) and “winter” (RMS error = 1.96°C). S9 exhibits a pattern of consistent levels of error through “summer” (RMS error = 1.46°C), “autumn” (RMS error = 1.43°C) and “winter” (RMS error

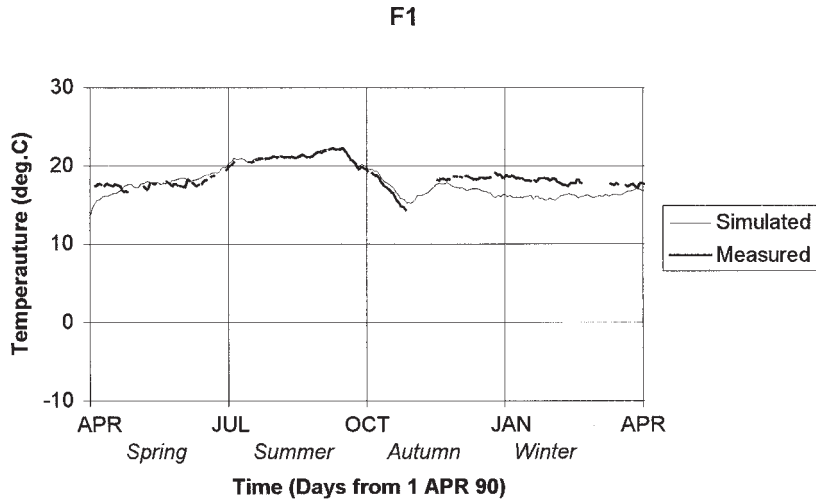


Figure 6.
Daily mean simulated and measured temperatures (node F1)

= 1.40°C) (Figure 9), with relatively weaker overall performance than F1. Nodes S1 and S5 (Figures 7 and 8) perform in a similar manner to each other with good “summer” (RMS error = 0.67°C and 0.43°C respectively) and “winter” (RMS error = 0.78°C and 0.46°C respectively) agreement but poorer “autumn” performance (RMS error = 1.54°C error and 1.21°C respectively). Essentially then, during the “summer” period of main interest, the F1 predictive performance is at its best. The errors for S1 and S5 begin to increase towards the end of this period whilst the errors for S9 remain relatively static.

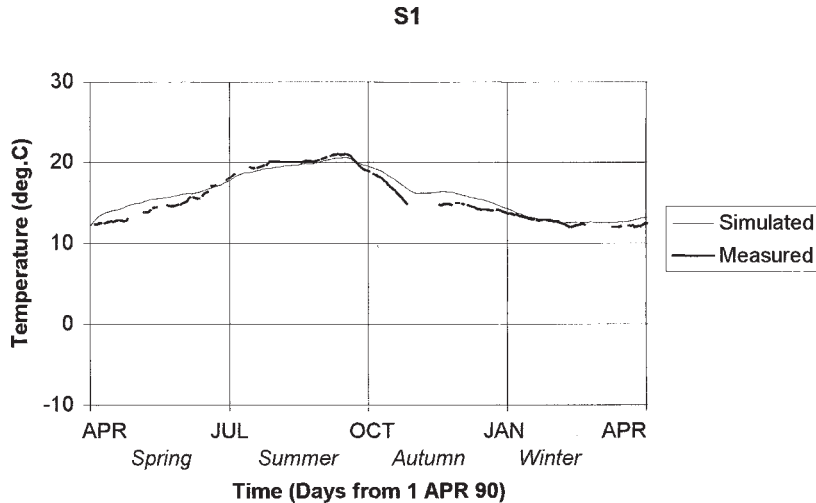


Figure 7.
Daily mean simulated and measured temperatures (node S1)

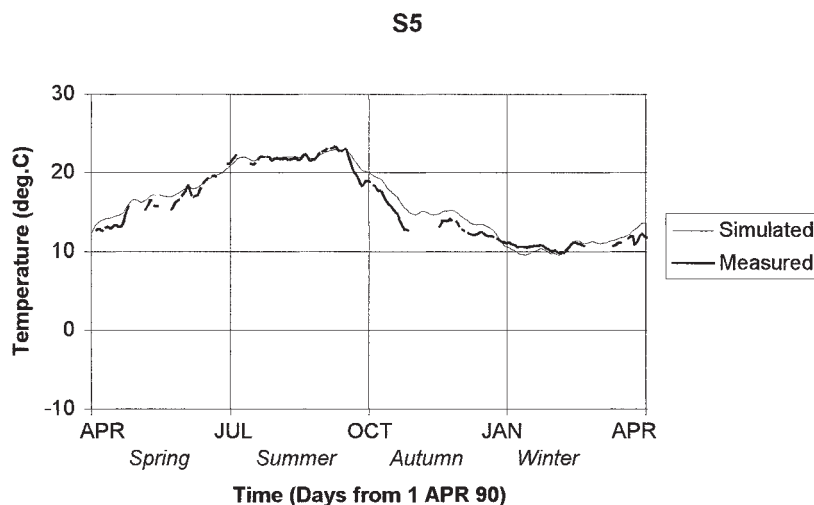


Figure 8.
Daily mean simulated and measured temperatures (node S5)

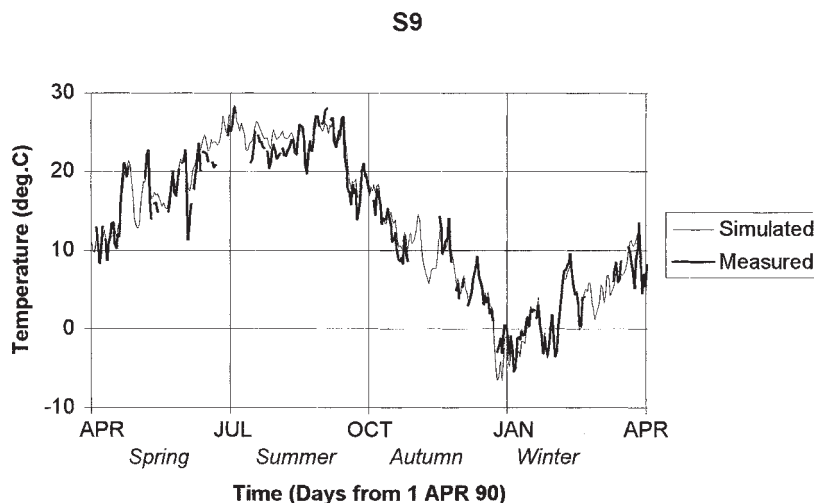


Figure 9.
Daily mean simulated and measured temperatures (node S9)

Analysis of results

In an attempt to investigate the source of the above errors, two main possible causes were investigated. These were the uncertainties in the input data and the effects of rainfall and snow coverage.

Input data – differential sensitivity analysis

There are inevitably relatively large uncertainties associated with assigning a particular soil type with constant values for its thermophysical parameters. These parameters will vary with moisture content, temperature, depth, etc. and thus it is vital to assess the predictive errors associated with these

uncertainties. A sensitivity study performed as part of this project by Adjali *et al.* (1998) showed that for the APACHE simulation of the FTF module, the conductivity of the soil was the most sensitive parameter. Thus in this section the results of a Differential Sensitivity Analysis (DSA) (Lomas and Eppel, 1991) are presented with regard to this property. The procedure involved in DSA is essentially simple. It is generally assumed when using this technique that each input parameter is distributed normally around the base-case value. If one then performs simulations with a particular input parameter set to values estimated to be a certain number of standard deviations removed from the base case values, then there is a definite probability that uncertainties in the input parameter could lead to changes greater than was observed in the predicted value.

For example, by performing runs with the parameters set to values estimated to be 2.33 standard deviations removed from the base-case there is only approximately a 1 per cent probability that uncertainties in the input could lead to changes greater than Δp (predicted value using base case inputs – predicted value using modified inputs) in the predicted value.

This process is then repeated for other input parameters. The resulting effects upon the predicted values are then grouped into those effects which increase the predicted value and those effects which decrease the predicted value. Provided that all the input parameters have been altered by the same amount, it is possible to combine these individual effects in quadrature to obtain an overall estimate of the range of predicted values which could occur as a result of the uncertainties in individual parameters.

Thus an hourly “allowable” error envelope can be built up (ultimately relating to all parameters used in the simulation). If the actual error lies within this envelope then the model may be performing correctly. If the actual error is outside this envelope then an “error” probably exists within the program.

Two assumptions are implicit in the above description of the technique:

- (1) That the effects of input uncertainties on the outputs are superposable over the range of input changes being considered i.e. that the sensitivity to each individual input is independent of the value of the other inputs.
- (2) The model is linear with respect to its input parameters.

These requirements will generally not be met exactly. However, work by Lomas and Eppel (1991) has shown that such assumptions may be reasonable and that agreement with the more sophisticated Monte Carlo Analysis technique is generally close.

Note that only the soil conductivities have been investigated in this present study and thus the error would be larger if all the parameters were taken into account. However, the envelopes presented here give a useful indication of the errors associated with uncertainties in the critical parameter of soil conductivity. Sixteen different soil conductivities are used in the simulation and so 32 runs were necessary to perform the analysis. The results are presented in Figures 10 to 13.

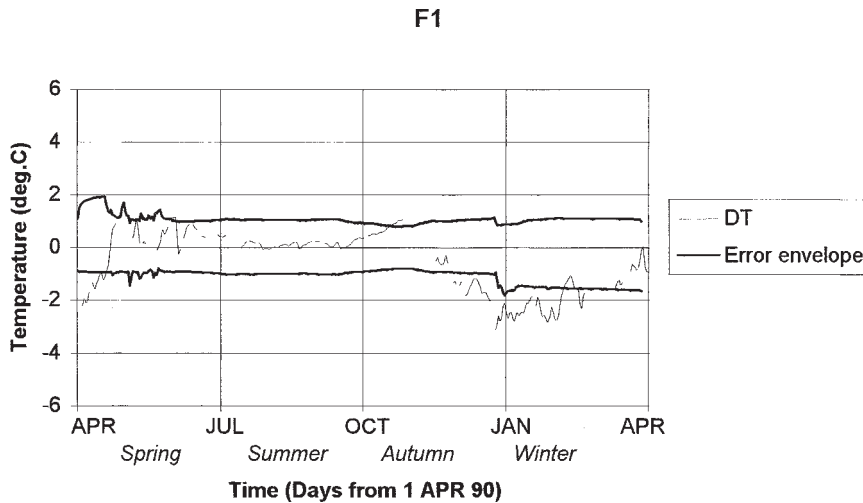


Figure 10.
Results of DSA study
(node F1)

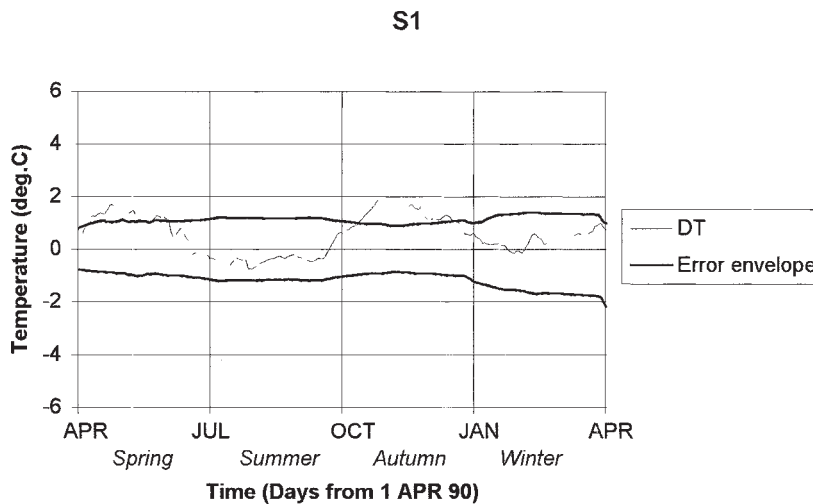


Figure 11.
Results of DSA study
(node S1)

Note that:

- In all cases a band of $\pm 0.75^{\circ}\text{C}$ has been added to allow for experimental errors associated with the thermocouple system.
- DT refers to (simulated temperatures – experimental data).

It can be seen that for node F1, the allowable envelope accounts for the error for all of the year other than the “winter” period. Here the actual error lies outside the envelope. For both the nodes S1 and S5, the “summer” and “winter” error is accounted for by the envelope. However, in the “autumn” the errors lie outside this envelope. For node S9 the envelope only accounts for the actual error

Figure 12.
Results of DSA study
(node S5)

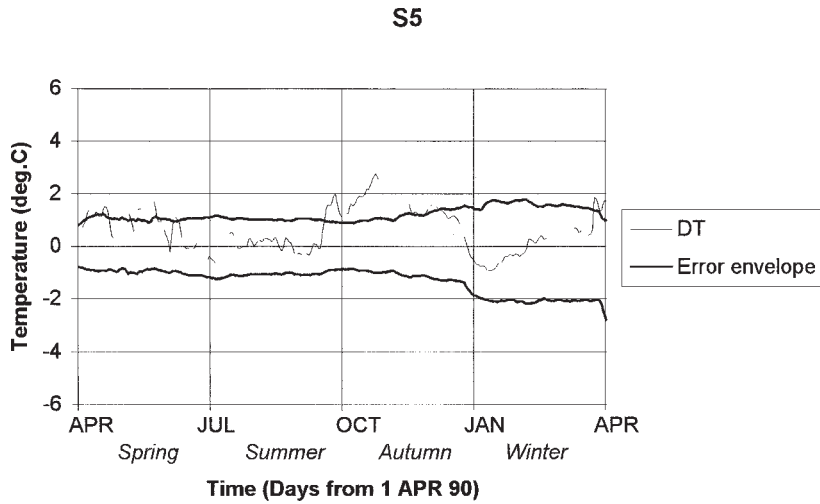
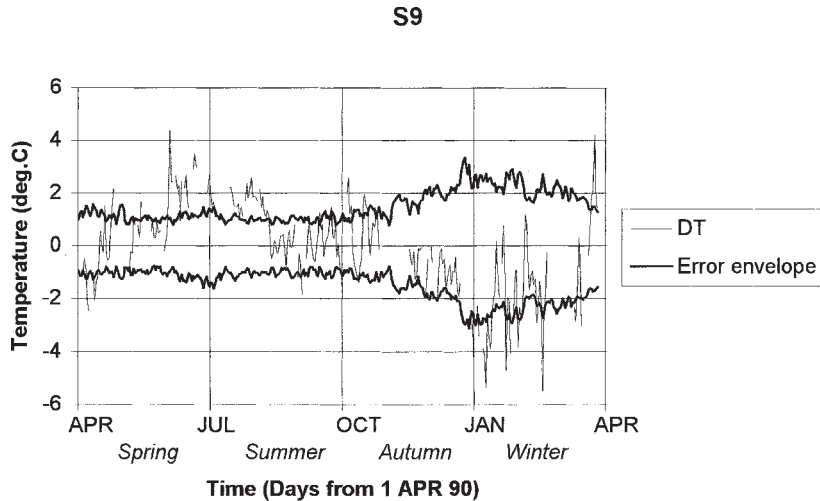


Figure 13.
Results of DSA study
(node S9)



during the “autumn” period. Note however that the size of the envelope for all nodes will be increased by the inclusion of other parameters.

The effects of rainfall and snow coverage

As mentioned previously, the basic numerical model cannot model moisture transfer or snow coverage. In an attempt to investigate this as a possible cause of the modelling errors reported above, daily precipitation and snow depth were plotted against these errors (Figures 14 and 15). Node S9 being close to the ground surface and node F1 being close to the floor surface were thought to be the most likely nodes to exhibit correlation with periods of rainfall and snow coverage. Note that in the case of F1 this was true because even though

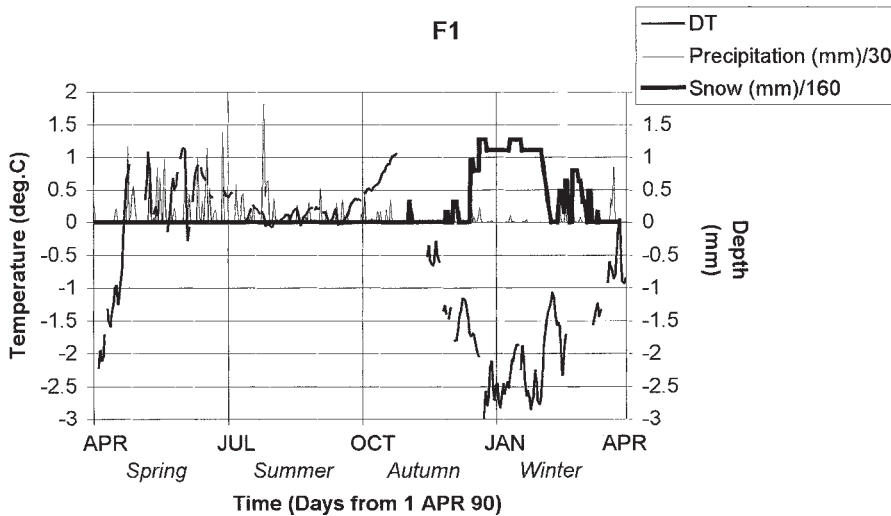


Figure 14. Rain and snow data plotted against error (node F1)

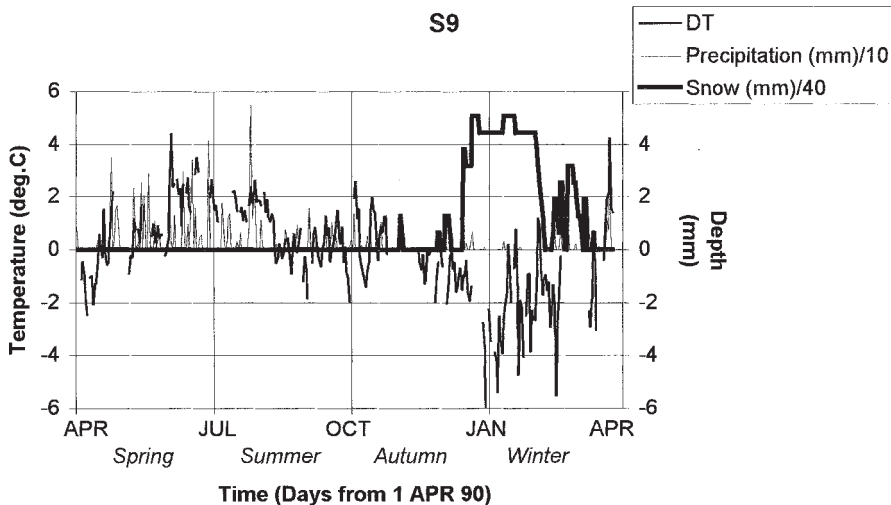


Figure 15. Rain and snow data plotted against error (node S9)

measured air temperatures were being used as internal boundary conditions, the internal radiant point was being calculated due to lack of measured data. It is clear that the periods of maximum error for nodes F1 and S1 correlate with the occurrence of rainfall or snow coverage. For both nodes, DT is positive in the “summer” and negative in the “winter”. Due to the observed correlation, it is proposed that this is (at least partially) explained as follows: in the “summer” the rainfall effectively lowers the temperature of the soil as compared to the simulated data which are not modelling this influence. In the “winter”, the soil acts as an insulating layer, not allowing the experimental data to fall to the

temperatures predicted by the model which is not including the effect of a snow layer. The influence of the snow seems to lead to larger errors than the influence of rainfall. No obvious correlation was observed for S1 and S5. This was not unexpected as they are both deep and removed from the room but the effect may have been compensated for by errors resulting from other sources (e.g. thermophysical properties). Thus the error for these nodes during the “autumn” period is more difficult to explain solely in terms of a short term response to rain fall or snow depth. Note that the model cannot take into account transpirative or evaporative effects and this will inevitably lead to predictive errors.

Conclusion

Summary

The results of the testing of a numerical model against measured data were presented. Due to the need for a pre-conditioning period and the model’s inability to deal with snow coverage, the “summer” period was the main period of interest for this study. For node F1 good agreement is achieved in the “summer”, but agreement is poorer in “winter”. Nodes S5 and S1 perform in a similar manner to each other with good “summer” and “winter” agreement but poor “autumn” performance. The errors for S9 remain relatively static throughout the year with an overall weaker performance than the other nodes.

Two possible sources of these errors were investigated: uncertainties in the input data and the effects of rainfall and snow coverage. In order to assess the importance of uncertainties in the model input data, a DSA study was performed. The study showed that uncertainties in the soil’s conductivity, coupled with errors in the measured data, could alone account for large periods of simulated error for each node. However, several periods of error remained in which the error was significantly higher than at other times. Thus an attempt was made to correlate these periods of error with periods of rainfall or snow coverage. It was clear that the periods of maximum error for the nodes most closely coupled with these influences coincided with the occurrence of rainfall or snow coverage. There remained the “autumn” period for which the temperatures of nodes S1 and S5 were outside the DSA envelope and also did not correlate in the short term with rainfall or snow depth. This effect may have been compensated for by errors resulting from other sources (e.g. thermophysical properties) and the non-treatment of transpirative and evaporative effects.

Conclusion 1

Modelling errors are introduced as a result of the non-treatment of the rainfall and snow coverage. The influence of the snow appears to be more significant.

Conclusion 2

Neither the non-treatment of the rainfall and snow coverage nor uncertainties in the most sensitive thermophysical parameter (the conductivity of the 16

soils) can explain errors in the modelled temperatures of nodes S1 and S5 during the “autumn” period. Uncertainties in other thermophysical properties and the non-treatment of transpirative and evaporative effects will contribute to these errors.

Conclusion 3

A purely conductive model may be capable, given accurate input data, of satisfactorily predicting the transient temperature variations in the soil/concrete envelope surrounding this structure for the period of the year when no snow coverage is present. However, if one is to accurately model regions of earth-contact (particularly at shallow depths) in a climate in which rainfall and snow are significant then these influences should be explicitly modelled. The results of this next stage of the project will be reported at a later date.

Symbology

- c specific heat capacity (J/kgK)
- SR surface resistance of external surface ($\text{m}^2\text{K/W}$)
- T temperature ($^{\circ}\text{C}$)
- t time (s)
- α absorptivity of external surface
- ε emissivity of external surface
- λ thermal conductivity (W/mK)
- ρ density (kg/m^3)

References

- Adjali, M.H., Davies, M. and Littler, J. (1998), “Three-dimensional earth-contact heat flows: a comparison of simulated and measured data for a buried structure”, *Renewable Energy*, Vol. 15, pp. 356-9.
- Bahnfleth, W.P. (1989), “Three-dimensional modelling of heat transfer from slab floors”, Technical Manuscript, USA Construction Engineering Research Laboratory.
- Chartered Institution of Building Services Engineers (1986), *CIBSE Guide*, London.
- Claesson, J. and Hagentoft, C.E. (1991), “Heat loss to the ground from a building – I. General theory”, *Building and Environment*, Vol. 26 No. 2, pp. 195-208.
- Claridge, D.E. (1987), “Design methods for earth-contact heat transfer”, in Boer, K. (Ed.), *Advances in Solar Energy*, American Solar Energy Society, Boulder, CO, pp. 305-50.
- Davies, M. (1994), “Computational and experimental three-dimensional conductive heat flows in and around buildings”, PhD thesis, University of Westminster.
- Davies, M., Tindale, A. and Littler, J. (1994), “The addition of a 3-D heat flow module to APACHE”, *BEPAC Conference*, York, UK.
- Davies, M., Tindale, A. and Littler, J. (1995), “Importance of multi-dimensional conductive heat flows in and around buildings”, *Building Serv. Eng. Res. Technol.*, Vol. 16 No. 2, pp. 83-90.
- Davies, M.G. (1990), “Room heat needs in relation to comfort temperatures: simplified calculation methods”, *Building Serv. Eng. Res. Technol.*, Vol. 11 No. 4, pp. 123-39.

-
- Farouki, O.T. (1986), "Thermal properties of soils", *Series in Rock and Soil Mechanics*, Vol. 11 trans., Tech Publications, Germany.
- Lloyd, R.M. (1994), "The influence of ground conditions on heat losses through floor slabs – an investigation of real behaviour factual report – HLTFS3 – results", University of Wales College of Cardiff.
- Lomas, K.J. and Eppel, H. (1991), "Developing and proving sensitivity analysis techniques for thermal simulation of buildings", *BEPAC Conference*, Canterbury, UK.
- Mihalakakou, G, Santamouris, M., Asimakopoulos, D. and Argiriou, A. (1995), "On the ground temperature below buildings", *Solar Energy*, Vol. 55 No. 2, pp. 355-62.
- Muncey, R.W.R. and Spencer, J.W. (1978), "Heat flow into the ground under a house", *Proceedings of Energy Conservation in Heating, Cooling and Ventilating Buildings*, Vol. 2, pp. 649-60.
- Patankar, S. (1980), *Numerical Heat Transfer and Fluid Flow*, Hemisphere, New York, NY.
- Saxhof, B., Schultz, J.M. and Thomsen, K.E. (1993), "Thermal analysis of Danish low energy rowhouses for IEA SHC Task 13 'Advanced solar low energy buildings'", *Proceeding of the Innovative Housing Conference*, Canadian Department of Natural Resources, Vancouver.
- Shipp, P.H. (1983), "Basement, crawlspace, and slab-on-ground thermal performance", *Proceedings of the ASHRAE/DOE Conference on Thermal Performance of the Exterior Envelopes of Buildings*, Las Vegas, NV, pp. 160-79.
- Thomas, H.R. (1987), "Non-linear analysis of heat and moisture transfer in unsaturated soils", *Journal Eng. Mech.*, Vol. 113 No. 8, pp. 1163-80.
- Van Den Brink, G.J. and Hoogendoorn, C.J. (1983), "Ground water flow heat losses for seasonal heat storage in the soil", *Solar Energy*, Vol. 30 No. 4, pp. 367-71.
- Walton, G. (1987), "Estimating 3-D heat loss from rectangular basements and slabs using 2-D calculations", *ASHRAE Transactions*, Vol. 93 No. 1, pp. 791-7.